Loss of RIG-I leads to a functional replacement with MDA5 in the Chinese tree shrew

Ling Xu[a,1], Dandan Yu[a,1], Yu Fan[a], Li Peng[a], Yong Wu[a,b], and Yong-Gang Yao[a,b,c,2]

[a]Key Laboratory of Animal Models and Human Disease Mechanisms of the Chinese Academy of Sciences & Yunnan Province, Kunming Institute of Zoology, Kunming, Yunnan 650223, China; [b]Kunming College of Life Science, University of Chinese Academy of Sciences, Kunming, Yunnan 650204, China; and [c]Kunming Primate Research Center of the Chinese Academy of Sciences, Kunming Institute of Zoology, Chinese Academy of Sciences, Kunming 650223, China

Edited by Harmit S. Malik, Fred Hutchinson Cancer Research Center, Seattle, WA, and accepted by Editorial Board Member Ruslan Medzhitov August 9, 2016 (received for review March 29, 2016)

The function of the RIG-I-like receptors (RLRs; including RIG-I, MDA5, and LGP2) as key cytoplasmic sensors of viral pathogen-associated molecular patterns (PAMPs) has been subjected to numerous pathogenic challenges and has undergone a dynamic evolution. We found evolutionary evidence that *RIG-I* was lost in the Chinese tree shrew lineage. Along with the loss of *RIG-I*, both *MDA5* (*tMDA5*) and *LGP2* (*tLGP2*) have undergone strong positive selection in the tree shrew. tMDA5 or tMDA5/tLGP2 could sense Sendai virus (an RNA virus posed as a RIG-I agonist) for inducing type I IFN, although conventional RIG-I and MDA5 were thought to recognize distinct RNA structures and viruses. tMDA5 interacted with adaptor tMITA (STINGTMEM173/ERIS), which was reported to bind only with RIG-I. The positively selected sites in tMDA5 endowed the substitute function for the lost RIG-I. These findings provided insights into the adaptation and functional diversity of innate antiviral activity in vertebrates.

RIG-I | MDA5 | tree shrew | positive selection | functional replacement

In persistent struggle between host and virus, the evolution of the innate immune system is a pivotal turning point. When virus enters and replicates inside the host cells, host innate immunity, as the first line of immune system to defense against pathogen infection, is quickly motivated. Host proteins, such as the germline-encoded pattern-recognition receptors (PRRs), which interact directly with viral protein, are subjected to molecular arms races (1). Cytosolic RIG-I-like receptors (RLRs), encompassing RIG-I (retinoic acid-inducible gene I, also known as DDX58) (2), MDA5 (melanoma differentiation factor 5, also known as IFIH1) (3), and LGP2 (laboratory of genetics and physiology 2, also known as DHX58) (4), which act as PRRs detecting viral PAMPs, mainly sense viral RNA in the cytosol (5) and trigger a series of signal cascades that lead to the production of type I IFN and various cytokines (6–8). These proteins bear the imprint of the long-term evolutionary arms race against viral RNA and other molecules (9). RIG-I and MDA5 share similar signaling features and structural homology: with two N-terminal caspase-recruitment domains (CARDs), a DExD/H box RNA helicase domain, and a C-terminal repressor domain (RD), whereas LGP2 lacks a CARD (2, 4, 10). The role of RIG-I and MDA5 in response to virus stimulation is not redundant: MDA5 specifically recognizes *Picornaviruses*, such as the encephalomyocarditis virus (EMCV), and RIG-I recognizes a wide variety of RNA viruses belonging to the *Paramyxovirus* and *Rhabdovirus* families (11). In contrast to MDA5 and RIG-I, the role of LGP2 in cytosolic RNA sensing remains controversial. Some reports suggested that LGP2 is essential for the production of type I IFN in response to several RIG-I– and MDA5-dependent viruses (10), whereas others described LGP2 as a negative regulator of the RIG-I signaling (12).

Evolutionary studies have painted an intricate picture of how RLRs have arisen and functionally diversified based on the CARDs of RIG-I and MDA5 (9, 13–15), which are essential in triggering the IFN response (2). It has been suggested that the CARD domains have been gained by RIG-I and MDA5 in two separate events: the first domain being acquired before the duplication that developed RIG-I and MDA5 and the second domain gained after their divergence (13). Moreover, the two CARDs found at separate loci in the sea anemone *Nematostellavectensis* suggested that these CARDs might have occurred in these loci after the divergence of the chordates (14). A recent study showed that RLR and MAVS CARDs diversified in early deuterostomes, probably through a series of tandem, partial-gene duplication events (15). In contrast to the CARDs, the divergence of RIG-I, MDA5, and LGP2 have remained unresolved (16). Zou et al. (14) demonstrated that RIG-I diverged in the early deuterostomes, with LGP2 and MDA5 diverging later in the vertebrates, whereas Sarkar et al. (13) showed that LGP2 diverged in the early chordates, followed by the divergence of RIG-I and MDA5 in the tetrapods. Recently, Mukherjee et al. showed that the RLR-based immune system might arise with the emergence of multicellularity (9). Although MDA5 and LGP2 homologs were found in many teleost fishes, clear RIG-I homologs have only been identified in salmon and carp (17). RIG-I was absent in the chicken genome, although MDA5 and LGP2 were both present (18, 19). The loss of RIG-I might affect the first line of defense at the lung epithelial cells during influenza infection in chickens. Therefore, it was not surprising that chickens suffer severely from avian influenza virus (AIV) infection compared with ducks (18). No mammalian species has been found to have a defective *RIG-I* until recently when we noted the absence of *RIG-I* in the Chinese tree shrew (*Tupaia belangeri chinensis*)

Significance

RIG-I-like receptors (RLRs) belong to a family of DExD/H box RNA helicases and comprise three members: RIG-I, MDA5, and LGP2. The function of RLRs as key cytoplasmic sensors of pathogen-associated molecular patterns has been subjected to numerous pathogenic challenges and undergone dynamic evolution, making it an excellent example for studying innate immunity evolution. We characterized the loss of RIG-I and found that tMDA5 acted as the pattern-recognition receptor responsible for sensing Sendai virus infection in the tree shrew, with an involvement of tLGP2 and tMITA. The positively selective sites in tMDA5 were crucial for the tMDA5-mediated antiviral signaling pathway. Our results provided insights into the evolutionary adaptation and functional diversity of antiviral activity in vertebrates.

Author contributions: L.X., D.Y., and Y.-G.Y. designed research; L.X., D.Y., Y.F., and L.P. performed research; L.X., D.Y., Y.F., Y.W., and Y.-G.Y. analyzed data; and L.X., D.Y., and Y.-G.Y. wrote the paper.

The authors declare no conflict of interest.

This article is a PNAS Direct Submission. H.S.M. is a Guest Editor invited by the Editorial Board.

[1]L.X. and D.Y. contributed equally to this work.

[2]To whom correspondence should be addressed. Email: yaoyg@mail.kiz.ac.cn.

This article contains supporting information online at www.pnas.org/lookup/suppl/doi:10.1073/pnas.1604939113/-/DCSupplemental.

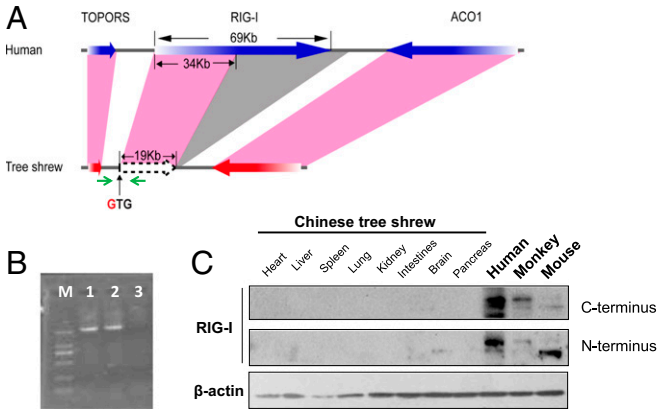

Fig. 1. RIG-I is absent in the Chinese tree shrew. (*A*) Diagram illustrating the structure of the tree shrew *RIG-I* genomic region. Color codes: pink shading, homologous genes from human to tree shrew; gray shading, tree shrew *RIG-I* deficient region relative to human alignment. The green arrows indicated the primers for amplifying the fragment containing the predictive start codon of the *RIG-I* gene. (*B*) PCR amplification of the *RIG-I* gene fragment using the cDNAs of human HeLa (lane 1), Malayan flying lemur (lane 2) cells, and Chinese tree shrew primary renal cells (lane 3). Lane M refers to DNA ladder. (*C*) Western blot showing the RIG-I protein in human, monkey, mouse, and Chinese tree shrew tissues. RIG-I antibodies recognized the C terminus and the N terminus of RIG-I, respectively.

genome (20). An understanding of the biological effects of the loss of RIG-I in the tree shrew will undoubtedly offer insights into the origin and development of the innate immunity in mammals.

In this study, we performed an evolutionary analysis and a functional characterization of the loss of *RIG-I* in the Chinese tree shrew. We confirmed that the absence of RIG-I in the tree shrew lineage, which accompanying with the presence of a positive selection signal on the other two RLR members, the tree shrew MDA5 (tMDA5) and LGP2 (tLGP2). Functional assays have shown that tMDA5 or tMDA5 combined with tLGP2 (tMDA5/tLGP2) could sense Sendai virus (SeV), which is a RIG-I agonist. tMDA5 could also interact with adaptor tMITA (21–23), which was reported to specifically bind with RIG-I. These results have suggested tMDA5 can replace or at least partially replace the function of RIG-I to sense RNA virus and enhance signaling via interaction with tMITA.

Results

RIG-I Is Absent in the Chinese Tree Shrew. An inspection of the Chinese tree shrew genome (20) revealed the *RIG-I* gene has been severely damaged so that functional RIG-I protein cannot be made (Fig. 1*A*). We identified the mutational change affecting the start codon of *RIG-I*, with the expected methionine-codon being replaced by a valine-codon (Fig. S1), in all 52 Chinese tree shrews collected from different geographic regions (Fig. S1). The *RIG-I* transcript was missing in tree shrew, but was expressed in both Malayan flying lemur (which has a close affinity to tree shrew) (24) and human cells (Fig. 1*B*). The RIG-I protein could be detected in human, monkey, and mouse, but not in tree shrew tissues (Fig. 1*C*). These results confirmed the loss of *RIG-I* in the tree shrew and showed this event occurred after the divergence of tree shrew from these other species.

A Substitute for the Lost RIG-I Acts as the Ligand of RNA Viruses and 5′ Triphosphate RNA. The absence of RIG-I in tree shrew has led us to hypothesize that the functioning of its antiviral innate immune system would be affected. Indeed, we observed different time-dependent expression patterns of *IFNB1* mRNA in tree shrew primary renal cells (TSPRCs) and HEK293 cells in response to Newcastle disease virus (NDV) infection (Fig. S2*A*). We further assessed the *tIFNB1* mRNA levels in TSPRCs challenged by a set of negative-sense RNA viruses, including SeV, AIV and VSV (vesicular stomatitis virus), and found that these viruses also significantly induced the *tIFNB1* mRNA expression (Fig. 2*A*). When TSPRCs were overexpressed with human RIG-I (hRIG-I; Fig. S2*B*), followed by infection of RNA viruses, the *tIFNB1* mRNA level was significantly up-regulated earlier than in the mocked cells (Fig. 2*A*). This observation suggested that loss of *RIG-I* in tree shrew had not suppressed, but only delayed the *tIFNB1* mRNA expression, and overexpression of hRIG-I had the compensatory effect. Evidently, there is an alternative sensor that recognizes RNA viruses and induces an antiviral response in TSPRCs. It is well established that RIG-I mediates antiviral response to RNAs bearing 5′ triphosphate RNA (5′ ppp RNA) (25); we therefore transfected 5′ ppp dsRNA into HeLa cells and TSPRCs. Owing to the presence of RIG-I in HeLa cells, the 5′ ppp dsRNA quickly induced the *IFNB1* mRNA expression and reached a high level at 6 h (Fig. 2*B*). In contrast, the 5′ ppp RNA had a delayed stimulation, with a slight effect at 6 h, significantly increased the *tIFNB1* mRNA levels at 12 h in TSPRCs (Fig. 2*B* and Fig. S2*C*). Similar results were obtained when SeV viral RNA

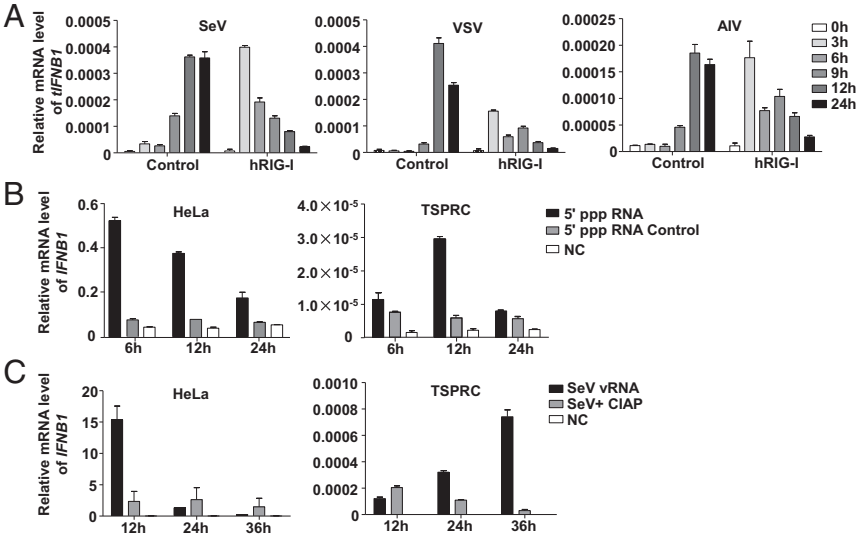

Fig. 2. A functional substitute for the lost RIG-I as the ligand of RNA viruses and 5′ triphosphate RNA (5′ ppp RNA) in TSPRCs. (*A*) Overexpression of human RIG-I (hRIG-I) can advance *tIFNB1* mRNA expression in response to different viral infections in TSPRCs. Cells (1×10^5) were transfected with hRIG-I expression vector or empty vector (1 μg) for 24 h and then were infected by viruses for indicated times. The 5′ ppp RNA (*B*) and SeV vRNAs (*C*) up-regulate *IFNB1* mRNA expression in HeLa and TSPRCs with a different time-dependent pattern; 5′ ppp RNA (100 ng/mL), 5′ ppp RNA control (100 ng/mL), SeV RNAs (100 ng/mL), and CIAP-treated SeV RNAs (100 ng/mL) were transfected into 1×10^5 cells for the indicated times, respectively. The *IFNB1* mRNA expression was measured by qRT-PCR. Experiments were performed in duplicate. Data are representative of three independent experiments.

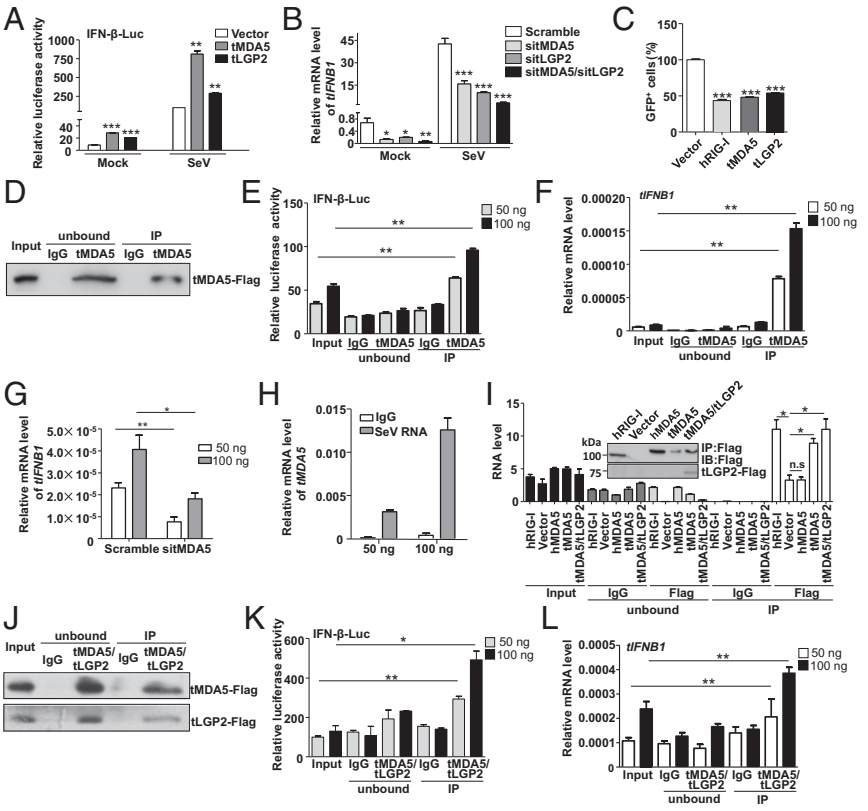

Fig. 3. tMDA5 or tMDA5/tLGP2 can sense SeV. (*A*) tLGP2 or tMDA5 activates the IFN-β-Luc reporter. TSPRCs (1×10^4) were transfected with IFN-β-Luc (100 ng), TK (10 ng), and expression vector for tLGP2 or tMDA5 (400 ng) for 36 h, and then were infected with SeV (20 HAU/mL) for 12 h before the luciferase assay. (*B*) Knockdown of tLGP2, tMDA5, or tLGP2/tMDA5 inhibits virus-induced *tIFNB1* mRNA expression. TSPRCs (1×10^5) were transfected with siRNA negative control (Scramble, 50 nM) or indicated siRNA (50 nM) for 24 h, followed by SeV infection for 12 h. (*C*) Overexpression of tLGP2 or tMDA5 inhibits VSV replication. TSPRCs (1×10^5) were transfected with equal amount of empty vector, hRIG-I, tLGP2, or tMDA5 expression vector (1 μg) for 12 h, followed by VSV-GFP (MOI = 0.01) infection for 12 h. Proportion of the GFP-positive cells was quantified by flow cytometry. (*D–F*) tMDA5 pull-down captures agonistic RNA from SeV-infected cells. About 1×10^8 TSPRCs were transfected with 30 μg FLAG-tagged tMDA5 expression vector and were cultured for 24 h and then infected with SeV for 16 h, followed by immunoprecipitation assays. Precipitation efficiency was verified by immunoblotting with an anti-Flag antibody (*D*). The RNAs from SeV-infected Flag-tMDA5-overexpressing TSPRCs (input), RNAs associated with tMDA5 or IgG immunoprecipitation (IP), or RNAs remaining after tMDA5 or IgG precipitations (unbound) were tested for the ability to stimulate the IFN-β-Luc activity in HEK293 cells (*E*) and to induce *tIFNB1* mRNA in TSPRCs (*F*). (*G*) Effect of the tMDA5-associated SeV RNAs was dependent on tMDA5. TSPRCs (1×10^5) were transfected with the indicated siRNA (50 nM) for 24 h and then transfected with the indicated amount of SeV RNAs for 6 h for measuring *tIFNB1* mRNA levels by qRT-PCR. (*H*) Up-regulation of *tMDA5* mRNA level by tMDA5-associated immunoprecipitated SeV RNAs in a dose-dependent manner. TSPRCs (1×10^5) were transfected with the indicated amount of SeV RNAs for 6 h. (*I*) Quantification of viral RNA bound by the Flag-tagged proteins from SeV-infected TSPRCs. (*Top*) Immunoblots showing Flag-tagged hRIG-I, hMDA5, tMDA5, and tMDA5/tLGP2 in IP. (*Bottom*) SeV RNA level was measured by the strand-specific qRT-PCR in vector, hRIG-I, hMDA5, tMDA5, tMDA5-tLGP2, and IgG immunoprecipitates. (*J–L*) tLGP2 enhances the ability to sense SeV by tMDA5 in TSPRCs. The procedures were similar to *D–F*. Data are representative of three independent experiments. $^*P < 0.05$, $^{**}P < 0.01$, $^{***}P < 0.001$, Student *t* test. Bars represent mean ± SEM.

(vRNA) was transfected in these cells. The SeV vRNA induced *IFNB1* mRNA to a high level in HeLa cells at 12 h but had a slow up-regulation effect in TSPRCs (Fig. 2*C*). However, when SeV vRNAs were treated with CIAP (to ablate the 5′ ppp ends), it had a weak effect on the *IFNB1* mRNA levels in both cells (Fig. 2*C*). These results suggested that human and tree shrew cells are different in sensing SeV vRNA, and there is a functional substitute for the loss of *RIG-I* in sensing these RNAs in the Chinese tree shrew.

Tree Shrew Cells Sensed SeV Through tMDA5, with an Involvement of tLGP2. We next sought to identify the cytosolic recognition elements in TSPRCs, which could replace the RIG-I function as the ligand of virus RNA. We found that the two members of RLRs, *tMDA5* and *tLGP2*, had a significantly increased mRNA expression after AIV, SeV, VSV, NDV, EMCV, or HSV-1 (herpes simplex virus-1) infection for 6 h or even later (Fig. S3*A*). Overexpression of tMDA5 and tLGP2 (Fig. S3*B*) significantly potentiated the virus-triggered activation of tIFN-β promoter luciferase (IFN-β-Luc) reporter activity (Fig. 3*A*), whereas knockdown of tMDA5 and tLGP2 (Fig. S3*B*) displayed the opposite effect (Fig. 3*B*). Moreover, as indicated by the diminished GFP expression, overexpression of tMDA5 and tLGP2 inhibited GFP-tagged VSV replication, with a comparable effect to that of hRIG-I overexpression (Fig. 3*C* and Fig. S3*C*). In addition, *tIFNB1* mRNA expression increased in TSPRCs on EMCV infection (Fig. S3*D*). Overexpression of tMDA5 markedly activated the EMCV-induced IFN-β-Luc, NF-κB-Luc, and ISRE-Luc reporters (Fig. S3*E*). Knockdown of tMDA5 and/or tLGP2 significantly inhibited EMCV-induced *tIFNB1* mRNA expression (Fig. S3*F*). These observations indicated that the function of tMDA5 and tLGP2 was homologous to that of the other mammals and had an obvious antiviral activity.

To confirm that tMDA5 was involved in the IFN-β response to SeV and acted as the RIG-I functional substitute, we used previously reported immunoprecipitation (IP) method (26, 27) to isolate tMDA5-associated RNA from SeV-infected cells. We first immunoprecipitated tMDA5 from SeV-infected TSPRCs transiently overexpressing a Flag-tagged tMDA5 protein (Fig. 3*D*), and then we extracted RNA from the precipitates and analyzed its stimulatory activity on the induction of IFN-β (Fig. 3 *E* and *F*). Notably, RNA associated with the tMDA5 precipitates (which contained SeV-derived vRNA; Fig. S4*A*), but not with the control (IgG) precipitates, stimulated the IFN-β-Luc reporter in HEK293 cells (Fig. 3*E*) and induced *tIFNB1*mRNA expression in TSPRCs (Fig. 3*F*). Moreover, knockdown of tMDA5 inhibited the immunoprecipitated SeV RNA-induced activation of the *tIFNB1* mRNA expression in TSPRCs (Fig. 3*G*). Immunoprecipitated SeV RNA induced *tMDA5* mRNA expression in a dose-dependent manner in TSPRCs (Fig. 3*H*). In human cells, RIG-I specifically bound the defective interfering (DI) particle during SeV infection (27). We used the strand-specific quantitative RT-PCR (qRT-PCR) with primers for SeV DI particle to validate the RNA associated with tMDA5 precipitates. We confirmed that tMDA5, but not human MDA5 (hMDA5), bound SeV RNA (Fig. 3*I*). tMDA5 had a weaker ability to bind SeV RNA than hRIG-I (Fig. 3*I*). In addition, we also found that tMDA5 had a higher binding affinity to the L region of EMCV compared with hRIG-I (Fig. S4*B*), and EMCV RNA was sufficient to trigger the MDA5-dependent IFN response (Fig. S4*C*). These results indicated that tMDA5 maintained its

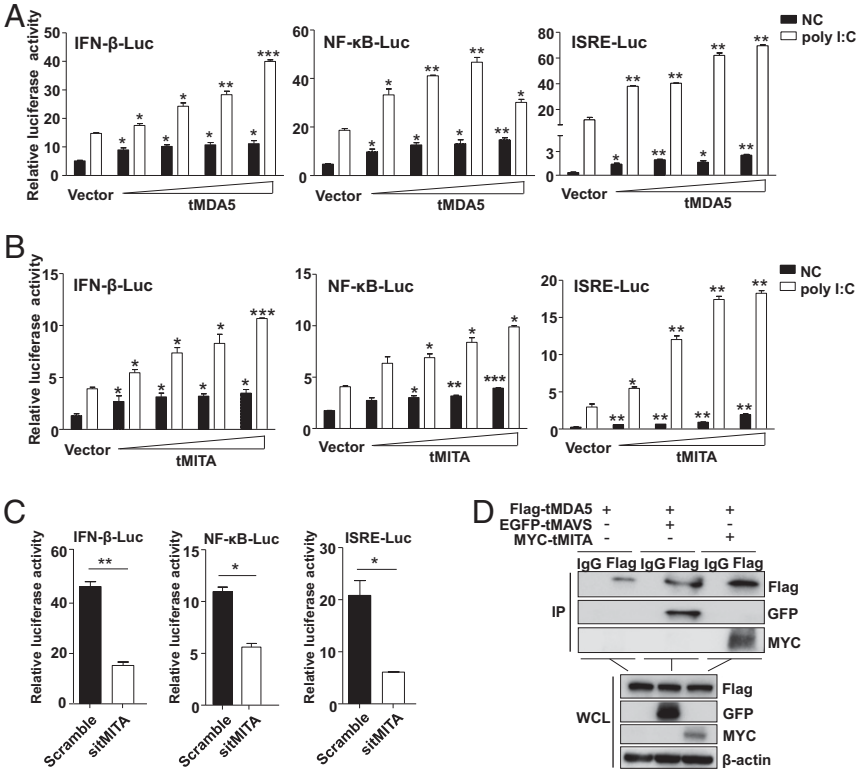

Fig. 4. tMDA5 interacts with tMITA in TSPRCs. Overexpression tMDA5 (*A*) and tMITA (*B*) activate the IFN-β-Luc, NF-κB-Luc, and ISRE-Luc reporters in a dose-dependent manner. Cells (1×10^4) were transfected with the respective reporter vector (100 ng), TK (10 ng), and increased amount (0, 3.2, 16, 80, and 400 ng) of tMDA5 or tMITA expression vector (with empty vector to reach a total amount of 400 ng) for 36 h and then were transfected with poly I:C (1 μg/mL) for 12 h. (*C*) Knockdown of tMITA causes an inhibition of poly I:C-induced IFN-β-Luc, NF-κB-Luc, and ISRE-Luc activities. (*D*) tMDA5 immunoprecipitates with tMITA. Cells (1×10^7) were cotransfected with MYC-tMITA (10 μg) and Flag-tMDA5 (10 μg) expression vectors for 36 h and then were infected with SeV for 16 h, followed by immunoprecipitation (IP) with anti-Flag, anti-MYC, or mouse IgG (control). The EGFP-tagged tMAVS was used as a positive control. Data are representative of three independent experiments. $*P < 0.05$, $**P < 0.01$, $***P < 0.001$, Student *t* test. Bars represent mean ± SEM.

original function to recognize EMCV and had evolved an additional function for the loss of RIG-I.

The LGP2 can assist MDA5-RNA interactions and leads to enhanced MDA5-mediated antiviral signaling (26, 28). Inclusion of tLGP2 significantly increased the tMDA5-dsRNA interaction at a lower concentration, but inhibited the tMDA5 signaling at a high level (Fig. S4*D*) (28). Transfection with low- or high-molecular-weight poly I:C up-regulated the *tIFNB1* mRNA expression (Fig. S4*E*), whereas *tMDA5* and *tLGP2* knockdown abolished this induction effect (Fig. S4*F*). These results suggested that TSPRCs sensed poly I:C through tMDA5, with a modification effect from tLGP2. We cotransfected tLGP2 and tMDA5 to immunoprecipitate tMDA5/tLGP2-associated RNA and analyzed the stimulatory activity of the precipitated RNAs. Consistent with the above results, tMDA5/tLGP2-associated RNAs could induce the IFN-β-Luc activity and *tIFNB1* mRNA expression (Fig. 3 *J–L*) and had a slightly higher binding affinity than tMDA5 alone (Fig. 3*I*), indicating that tLGP2 was able to synergize with tMDA5 to render cells to be more sensitive to SeV infection, finally leading to an enhanced tMDA5-mediated antiviral signaling.

tMDA5 Interacted with tMITA. MITA preferentially modulated the RIG-I-, rather than the MDA5-signaling (21, 22). MITA was unable to mediate the signaling triggered by high-molecular-weight poly I:C (poly I:C H), which was known to be sensed by MDA5 (Fig. S4*F*) (23, 29). To examine whether tMDA5 could replace RIG-I to interact with tMITA, we overexpressed tMDA5 and tMITA in TSPRCs separately and investigated the activation effect of the IFN-β-Luc, NF-κB-Luc, and ISRE-Luc reporters in response to poly I:C. Both tMDA5 and tMITA could induce the IFN-β-Luc, NF-κB-Luc, and ISRE-Luc activities in a dose-dependent manner in response to poly I:C H (Fig. 4 *A* and *B* and Fig. S5*A*), and tMITA was a downstream mediator of the tMDA5 signaling (Fig. S5*B*). Knockdown of endogenous tMITA (by sitMITA; Fig. S5*C*) inhibited the activation of the IFN-β-Luc, NF-κB-Luc, and ISRE-Luc by poly I:C H (Fig. 4*C*). These results suggested that tMITA mediated the tMDA5-dependent signaling triggered by poly I:C H. Coimmunoprecipitation showed that tMDA5 could interact with tMITA in SeV-infected TSPRCs (Fig. 4*D*). Taken together, tMDA5 can bind to tMITA in the absence of RIG-I and mediate the corresponding signaling in tree shrew.

***MDA5* and *LGP2* Underwent Positive Selection in the Tree Shrew Lineage.** To understand the evolutionary dynamics and selective pressure on the RLR genes in the tree shrew due to the loss of *RIG-I*, we used the branch models and the branch-site models based on the maximum-likelihood method implemented in the phylogenetic analysis by maximum likelihood (PAML) package (30) to calculate the average nonsynonymous substitution/synonymous substitution rate (d_N/d_S, also known as ω) for *MDA5* and *LGP2*. We first tested with the branch models, which were based on the model M0 with same ω for all branches and the model M2 with different ω on selected branches, and then we compared M0 and M2 by the likelihood ratio test (31). As shown in Table S1, *tMDA5* and *tLGP2* underwent a positive selection (*tMDA5*, $P = 0.032$; *tLGP2*, $P = 0.032$). The positive selections were further evaluated by using the branch-site models (32) implemented in PAML (30), which is powerful for detecting episodic positive selection and for generating biological hypotheses for mutation and functional analyses (33). Similar positive selection signature was detected in *tMDA5* ($P = 0.007$), whereas no significant sites were found for *tLGP2* ($P > 0.05$) (Table S1). In detail, the branch-site models analysis detected two positively selected residues (Lys188 and Ala402) in the tMDA5 (Table S1).

The Positively Selected Sites in tMDA5 Endowed the Substitute Function for the Lost RIG-I. To functionally characterize the potential selection effect on *tMDA5*, we focused on the two positively selected sites (PSSs) Lys188 and Ala402 in tMDA5, which were highly conserved in the primates (Table S1 and Fig. S6 *A* and *B*). Structural modeling showed that the equivalent positions of the

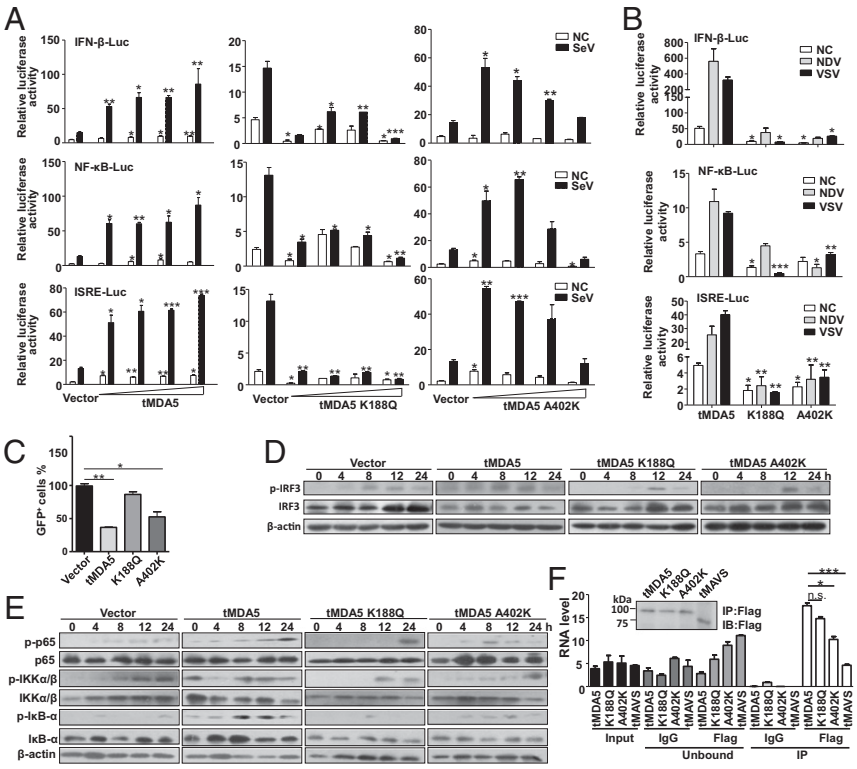

Fig. 5. Antiviral responses in tree shrew cells overexpressing tMDA5 and its mutants. (*A*) Different stimulatory effects of tMDA5, tMDA5 K188Q, and tMDA5 A402K on the activation of the IFN-β-Luc, NF-κB-Luc, and ISRE-Luc reporters in a dose-dependent manner. The procedures are same to Fig. 4*A*, except for SeV infection for 12 h. (*B*) Effects of overexpression of tMDA5, tMDA5 K188Q, and tMDA5 A402K on IFN-β-Luc, NF-κB-Luc, and ISRE-Luc reporters on NDV and VSV-GFP infections. Cells were transfected as *A*, except with 400 ng expression vector and different virus infections (NDV, MOI = 10; VSV-GFP, MOI = 0.01). (*C*) Different inhibition effects of tMDA5 and its mutants on VSV-GFP replication. (*D* and *E*) Effects of tMDA5 and its mutants on activation of phospho-IRF3, phospho-p65, phospho-IKKα/β, and phospho-IκBα. (*F*) Quantification of viral RNA bound by the Flag-tagged tMDA5 and its mutants from SeV-infected TSPRCs. The procedure and labels are the same as Fig. 3*I*. Data are representative of three independent experiments. $*P < 0.05$, $**P < 0.01$, $***P < 0.001$, Student *t* test. Bars represent mean ± SEM.

PSSs in tMDA5 are located in critical domains: the Lys188 is located in the second CARD near the helicase domain, which is essential for coupling to the downstream signaling adaptors (34); the Ala402 is located in the DECH box helicase domain (35) (Fig. S6 *A* and *C*). We located the PSSs based on the crystal structures of hMDA5 (Protein Data Bank ID code 4GL2) and found that Ala402 was adjacent to regions involved in dsRNA binding (35) (Fig. S6*D*). Alteration of basic amino acid lysine to neutral alanine at this position might have changed the affinity between dsRNA and tMDA5. Evidently, the in silico prediction analysis demonstrated that these PSSs were probably crucial for tMDA5-mediated antiviral signaling pathway.

To examine the potential function of the two PSSs in tMDA5, we swapped the Lys188 and Ala402 in tMDA5 back to the evolutionarily conserved and primitive glutamine (K188Q) and lysine (A402K), respectively (Fig. S6). tMDA5 induced the IFN-β-Luc, NF-κB-Luc, and ISRE-Luc activities in a dose-dependent manner by Mock or SeV induction, whereas tMDA5 K188Q robustly inhibited these luciferase activities. tMDA5 A402K only activated these reporters at a low concentration but decreased their activities at a high concentration on SeV infection (Fig. 5*A* and Fig. S7*A*). We speculated that this pattern was caused by different regulation effects of heterodimer of endogenous tMDA5 and exogenous tMDA5 A402K and homodimer of exogenous tMDA5 A402K in TSPRCs. Similarly, tMDA5 K188Q and tMDA5 A402K, but not tMDA5, had no apparent ability to activate the luciferase reporters in response to NDV and VSV infections (Fig. 5*B* and Fig. S7*B*). tMDA5 and tMDA5 A402K, but not tMDA5 K188Q, inhibited VSV replication, albeit with different capabilities (Fig. 5*C* and Fig. S7*C*). To further confirm the critical role of the PSSs of tMDA5, we performed a gain-of-function analysis by introducing mutations at the equivalent positions in hMDA5. We found that hMDA5 Q187K and K405A significantly potentiated the IFN-β-Luc, NF-κB-Luc, and ISRE-Luc activities induced by SeV and NDV in HEK293 and HepG2 cells, but no effect was observed for EMCV infection (Fig. S7 *D*–*F*). Thus, the role of hMDA5 mutants was consistent with that of tMDA5 (Fig. 5 *A* and *B* and Fig. S3*E*), suggesting that the two PSSs in MDA5 endowed tMDA5 a substitute function for the lost RIG-I. Note that both hMDA5 mutants have not been found in the general human populations (>60,000 individuals; *SI Materials and Methods*), suggesting both sites were extremely conserved.

We further assessed the antiviral activity of tMDA5 and its mutants by analyzing phosphorylation of the transcription factor IRF3 and NF-κB signaling. Infection with SeV induced phosphor-IRF3 in TSPRCs overexpressing tMDA5 and it mutants, but tMDA5 K188Q and tMDA5 A402K activated the phosphor-IRF3 at a later time point (12 h) (Fig. 5*D*). Concordantly, tMDA5 K188Q and tMDA5 A402K affected the ability of SeV to induce phospho-p65, phospho-IKKα/β, and phospho-IκBα, with a different pattern compared with tMDA5 (Fig. 5*E*). The RNA IP assay showed that tMDA5 A402K had a weaker ability to sense SeV RNA than tMDA5 and tMDA5 K188Q (Fig. 5*F* and Fig. S7 *G*–*L*). These results were consistent with the structure prediction that the PSSs K188 and A402 were located in different functional domains (Fig. S6) and affected the SeV-induced IRF3 and NF-κB activation.

Discussion

The RLR proteins play a key role in the innate immune system response against viral infection by recognizing viral RNA molecules (36, 37). RLRs are highly conserved during vertebrate evolution (13, 14), and loss of RIG-I in mammalian species is extremely rare (20). The loss of any RLR member might be expected to have a great impact on immune response. In this study, we characterized the consequences resulting from the loss of RIG-I in the tree shrew and provided direct functional evidence for the diversification of the RLR members in this species due to the inability to produce RIG-I. Accompanying this change, we observed a positive selection signal on tMDA5 and tLGP2. We found that tMDA5 alone or tMDA5/tLGP2 could replace RIG-I in sensing RNA viruses and trigger IFN production. This replacement might be enhanced by the interaction of tMDA5 with tMITA, which was proved to specifically interact with RIG-I to cascade the antiviral signaling (22). The functional divergence between tMDA5 and its mutants indicated that the

compensatory effect of tMDA5 might be driven by natural selection. Loss of RIG-I has resulted in a functional replacement by MDA5 or MDA5/LGP2 as a cytosolic RNA sensor to trigger IFN production.

Although the available data suggested that loss of RIG-I has led to MDA5 functional alteration, most likely via the PSSs in tMDA5, it raised an interesting question: the time order of RIG-I loss and the positive selection on MDA5—which one is earlier in the tree shrew? A straightforward explanation is that tMDA5 first mutated and evolved by positive selection to gain a new function to achieve the ability to sense the viruses that were initially recognized by RIG-I, and then the redundant RIG-I gradually eroded in the genome. This assumption would be compatible with the pattern for overlapped recognition of same viruses by both MDA5 and RIG-I (38). The RIG-I is essential for preferentially recognizes RNAs bearing 5′ ppp ends in vertebrates, which serve to define a nonself RNA PAMP (25, 36, 39). It was unlikely that tree shrew accidentally lost RIG-I, because the sudden loss of RIG-I would render this species be more susceptible to virus infections (11, 18, 40). Moreover, RLRs and their downstream signaling molecules could be found in the earliest animals, suggesting for an ancient origin of the RLRs (15). However, it remains a challenge to attribute the selection patterns of RLRs to virus-mediated natural selection in the tree shrew.

Besides MDA5, LGP2 acts as a regulator of RLR-mediated antiviral signaling and was reported to play apparently conflicting roles in different studies (10, 41). In contrast to negative regulation in the RIG-I-mediated signaling pathway (4, 42, 43), tree shrew cells lacking tLGP2 exhibited a decreased *IFNB1* mRNA expression in response to RNA virus infections (Fig. 3*B*). Moreover, tLGP2 could synergize with tMDA5 to sense SeV infection (Fig. 3*I*). This pattern is consistent with the observation that silencing endogenous chLGP2 reduced *chIFN-β* mRNA expression induced by AIV, suggested that chLGP2 had a positive role in antiviral signaling (19). Taken both observations in the tree shrew and chicken together, we speculated that LGP2 had a positive role in regulating the RLR signaling pathway upon the RIG-I loss, and this role was endowed by the evolution. One unresolved question arising from this study is that whether other immune genes would undergo similar effect upon the RIG-I loss, as we would anticipate a cascade event for the loss of this important factor.

In short, we uncovered a previously unknown evolutionary signal in response to RIG-I loss in the tree shrew. The loss of RIG-I was accompanied by a functional substitute with MDA5 involving LGP2, which underwent positive selection. Our study provides an example that will assist our understanding of the functional evolution and conservation of the innate immune system in vertebrates.

Materials and Methods

SI Materials and Methods and Table S2 contains complete related information in this study. All of the experimental procedures were performed according to the guidelines approved by the Institutional Animal Care and Use Committee of Kunming Institute of Zoology.

ACKNOWLEDGMENTS. We thank Ian Logan for language editing and Dr. Xuelong Jiang for sharing the tree shrew DNA samples. This study was supported by National Natural Science Foundation of China Grant U1402224.

1. Duggal NK, Emerman M (2012) Evolutionary conflicts between viruses and restriction factors shape immunity. *Nat Rev Immunol* 12(10):687–695.
2. Yoneyama M, et al. (2004) The RNA helicase RIG-I has an essential function in double-stranded RNA-induced innate antiviral responses. *Nat Immunol* 5(7):730–737.
3. Andrejeva J, et al. (2004) The V proteins of paramyxoviruses bind the IFN-inducible RNA helicase, mda-5, and inhibit its activation of the IFN-beta promoter. *Proc Natl Acad Sci USA* 101(49):17264–17269.
4. Yoneyama M, et al. (2005) Shared and unique functions of the DExD/H-box helicases RIG-I, MDA5, and LGP2 in antiviral innate immunity. *J Immunol* 175(5):2851–2858.
5. Baccala R, et al. (2009) Sensors of the innate immune system: Their mode of action. *Nat Rev Rheumatol* 5(8):448–456.
6. Takeuchi O, Akira S (2010) Pattern recognition receptors and inflammation. *Cell* 140(6):805–820.
7. Barbalat R, Ewald SE, Mouchess ML, Barton GM (2011) Nucleic acid recognition by the innate immune system. *Annu Rev Immunol* 29:185–214.
8. Ronald PC, Beutler B (2010) Plant and animal sensors of conserved microbial signatures. *Science* 330(6007):1061–1064.
9. Mukherjee K, Korithoski B, Kolaczkowski B (2014) Ancient origins of vertebrate-specific innate antiviral immunity. *Mol Biol Evol* 31(1):140–153.
10. Satoh T, et al. (2010) LGP2 is a positive regulator of RIG-I- and MDA5-mediated antiviral responses. *Proc Natl Acad Sci USA* 107(4):1512–1517.
11. Kato H, et al. (2006) Differential roles of MDA5 and RIG-I helicases in the recognition of RNA viruses. *Nature* 441(7089):101–105.
12. Bruns AM, Horvath CM (2012) Activation of RIG-I-like receptor signal transduction. *Crit Rev Biochem Mol Biol* 47(2):194–206.
13. Sarkar D, Desalle R, Fisher PB (2008) Evolution of MDA-5/RIG-I-dependent innate immunity: Independent evolution by domain grafting. *Proc Natl Acad Sci USA* 105(44):17040–17045.
14. Zou J, Chang M, Nie P, Secombes CJ (2009) Origin and evolution of the RIG-I like RNA helicase gene family. *BMC Evol Biol* 9(1):85.
15. Korithoski B, et al. (2015) Evolution of a novel antiviral immune-signaling interaction by partial-gene duplication. *PLoS One* 10(9):e0137276.
16. Lewis SH, Obbard DJ (2014) Recent insights into the evolution of innate viral sensing in animals. *Curr Opin Microbiol* 20(0):170–175.
17. Biacchesi S, et al. (2009) Mitochondrial antiviral signaling protein plays a major role in induction of the fish innate immune response against RNA and DNA viruses. *J Virol* 83(16):7815–7827.
18. Barber MRW, Aldridge JR, Jr, Webster RG, Magor KE (2010) Association of RIG-I with innate immunity of ducks to influenza. *Proc Natl Acad Sci USA* 107(13):5913–5918.
19. Liniger M, Summerfield A, Zimmer G, McCullough KC, Ruggli N (2012) Chicken cells sense influenza A virus infection through MDA5 and CARDIF signaling involving LGP2. *J Virol* 86(2):705–717.
20. Fan Y, et al. (2013) Genome of the Chinese tree shrew. *Nat Commun* 4:1426.
21. Zhong B, et al. (2008) The adaptor protein MITA links virus-sensing receptors to IRF3 transcription factor activation. *Immunity* 29(4):538–550.
22. Ishikawa H, Barber GN (2008) STING is an endoplasmic reticulum adaptor that facilitates innate immune signalling. *Nature* 455(7213):674–678.
23. Sun W, et al. (2009) ERIS, an endoplasmic reticulum IFN stimulator, activates innate immune signaling through dimerization. *Proc Natl Acad Sci USA* 106(21):8653–8658.
24. Murphy WJ, et al. (2001) Resolution of the early placental mammal radiation using Bayesian phylogenetics. *Science* 294(5550):2348–2351.
25. Hornung V, et al. (2006) 5′-Triphosphate RNA is the ligand for RIG-I. *Science* 314(5801):994–997.
26. Deddouche S, et al. (2014) Identification of an LGP2-associated MDA5 agonist in picornavirus-infected cells. *eLife* 3:e01535.
27. Baum A, Sachidanandam R, García-Sastre A (2010) Preference of RIG-I for short viral RNA molecules in infected cells revealed by next-generation sequencing. *Proc Natl Acad Sci USA* 107(37):16303–16308.
28. Bruns AM, Leser GP, Lamb RA, Horvath CM (2014) The innate immune sensor LGP2 activates antiviral signaling by regulating MDA5-RNA interaction and filament assembly. *Mol Cell* 55(5):771–781.
29. Abe T, Barber GN (2014) Cytosolic-DNA-mediated, STING-dependent proinflammatory gene induction necessitates canonical NF-κB activation through TBK1. *J Virol* 88(10):5328–5341.
30. Yang Z (2007) PAML 4: Phylogenetic analysis by maximum likelihood. *Mol Biol Evol* 24(8):1586–1591.
31. Nielsen R, Yang Z (1998) Likelihood models for detecting positively selected amino acid sites and applications to the HIV-1 envelope gene. *Genetics* 148(3):929–936.
32. Zhang J, Nielsen R, Yang Z (2005) Evaluation of an improved branch-site likelihood method for detecting positive selection at the molecular level. *Mol Biol Evol* 22(12):2472–2479.
33. Yang Z, dos Reis M (2011) Statistical properties of the branch-site test of positive selection. *Mol Biol Evol* 28(3):1217–1228.
34. Goubau D, Deddouche S, Reis e Sousa C (2013) Cytosolic sensing of viruses. *Immunity* 38(5):855–869.
35. Wu B, et al. (2013) Structural basis for dsRNA recognition, filament formation, and antiviral signal activation by MDA5. *Cell* 152(1-2):276–289.
36. Yoo JS, Kato H, Fujita T (2014) Sensing viral invasion by RIG-I like receptors. *Curr Opin Microbiol* 20:131–138.
37. Yoneyama M, Onomoto K, Jogi M, Akaboshi T, Fujita T (2015) Viral RNA detection by RIG-I-like receptors. *Curr Opin Immunol* 32:48–53.
38. Schoggins JW, et al. (2011) A diverse range of gene products are effectors of the type I interferon antiviral response. *Nature* 472(7344):481–485.
39. Loo YM, Gale M, Jr (2011) Immune signaling by RIG-I-like receptors. *Immunity* 34(5):680–692.
40. Yoneyama M, Fujita T (2010) Recognition of viral nucleic acids in innate immunity. *Rev Med Virol* 20(1):4–22.
41. Rodriguez KR, Bruns AM, Horvath CM (2014) MDA5 and LGP2: Accomplices and antagonists of antiviral signal transduction. *J Virol* 88(15):8194–8200.
42. Saito T, et al. (2007) Regulation of innate antiviral defenses through a shared repressor domain in RIG-I and LGP2. *Proc Natl Acad Sci USA* 104(2):582–587.
43. Rothenfusser S, et al. (2005) The RNA helicase Lgp2 inhibits TLR-independent sensing of viral replication by retinoic acid-inducible gene-I. *J Immunol* 175(8):5260–5268.
44. Yang Z, Wong WS, Nielsen R (2005) Bayes empirical bayes inference of amino acid sites under positive selection. *Mol Biol Evol* 22(4):1107–1118.